Temporal Dynamics of Mobile Blocking in Millimeter Wave Based Wearable Networks

Yicong Wang and Gustavo de Veciana
Department of Electrical and Computer Engineering, The University of Texas at Austin
Email: yicong.wang@utexas.edu, gustavo@ece.utexas.edu

***Abstract*—Wireless channels in millimeter wave based wearable networks are particularly susceptible to environmental blockages and dynamics when there are humans/objects in motion. Such dynamics imply, not only physical layer overheads to discover and track viable transmission paths, but also MAC overheads to keep track of neighboring interferers, perform clustering and enable proper scheduling of transmissions. We shall focus on overheads at timescale associated with the latter. This paper introduces a stochastic geometric model to study the impact of mobility on overheads in such networks. We provide a complete characterization of the temporal dynamics of strong interference channels resulting from blocking in networks comprising both fixed and mobile nodes. We show the state of a channel, Line-of-Sight(LOS)/Non-LOS(NLOS), follows an on/off renewal process and derive the associated distributions. Our model further enables us to evaluate how the overall rate of change for the set of strong LOS interferers seen by a fixed user scales with user density and proportion of mobile users. The overhead to track the interference environment may in fact be limited with user density but increases with proportion of mobile users. In a highly mobile environment, the changes in channels are frequent and the overheads for coordination become high, with distant and/or mobile users requiring more overheads. Based on our results, we suggest fixed users may coordinate with close by neighbors while mobile users are better off resorting to simpler ad hoc MACs.**

I. Introduction

Wearable devices are increasingly permeating our everyday lives [1]. It is expected that, in the near future, display and sensing devices enabling high quality augmented reality, tactile Internet, and/or high fidelity audio/video, might become common place. These applications and services require much higher bandwidths along with tight Quality of Service (QoS) guarantees, which are best met by enabling local connectivity (without clumsy wires) via millimeter wave (mmWave) based links. Indeed the mmWave band includes unprecedented swaths of available spectrum along with the opportunity to integrate arrays of antennas on small form factors which enable highly directional transmissions.

Directionality physical layer challenges. Acquiring and maintaining robust communication channels in mmWave bands is a recognized physical layer challenge. Many approaches to quickly acquiring and adapting beams are under study see e.g., [2], [3], [4]. There are also trade-offs between achieving high beamforming gains with narrow beams which may be quite sensitive to change/blockage and using more robust wider beams with lower gains and resulting in more interference to other devices. Thus although directionality provides a degree of isolation among neighboring receivers, it is still expected that MAC-based coordination and scheduling will be needed to meet the high bandwidth and QoS requirements of future applications. This is particularly the case in "worst case" dense and possibly dynamic indoor environments, e.g., in a crowded train car or airport, where users will still expect their devices to operate flawlessly.

MAC coordination and scheduling. In wearable networks, data transmissions might be for the most part amongst devices on the same user, thus aside from self-blocking, they are most impacted by interference from other users. To remedy this problem body network MACs can track neighbors with strong Line-of-Sight (LOS) interference channels permitting scheduling of transmissions. In addition, different users' body networks can exchange signaling messages to form clusters enabling even better coordination and scheduling of transmissions, see [5] and IEEE 802.11ad[6]. Unfortunately, frequent changes in channel state may degrade the effectiveness of coordination and increase MAC overheads associated with channel estimation and coordination.

Role of blocking and network dynamics. Characterizing the impact of network dynamics on mmWave networks is a challenging problem. Indeed although there may be a large numbers of users, and thus possible interferers, there is also increased blocking by human bodies which helps reduce the number of strong interferers [7][8]. Thus in this setting the MAC need only coordinate amongst a few close by interferers to improve the capacity and QoS [5]. Still, in dynamic settings, user mobility may result in an excessive rate of change that would be difficult for MAC schedulers to track. In particular the signal and interference paths are dominated by LOS channels, which could change frequently due to blockages in a dynamic environment. Such variations make it difficult to establish stable links for data transmission but also to properly track and schedule around strong neighboring interferers.

Contributions. To better understand and evaluate MAC designs for dense mmWave wearable networks with mobile users/blockages, it is important to answer the following two questions:

1) What is the intensity of variation of channel state in an environment with mobile users/blockages?
2) How do such variations impact signaling overheads of typical MAC protocols?

To answer these questions we first propose a first-order model, based on stochastic geometry, enabling the study of temporal

978-3-901882-90-6/17 ©2017 IFIP

channel variations, i.e., changing state between LOS and non-LOS (NLOS), in a mobile environment. We prove that the temporal variation follows an on/off renewal process. The duration of an on (LOS) period, is shown to be exponentially distributed whose mean is inversely proportional to the mobile user/blockage density, speed, and link length. We also show that the duration of off states (NLOS) can be approximated by an exponential distribution in dense and mobile scenarios. We then characterize the rate of change in channel states (LOS/NLOS) as seen by a typical fixed user to evaluate the cost associated with tracking and coordinating such changes. If the proportion of mobile users is fixed, the rate of change first increases with user density then saturates and decreases due to blockages. If user density is fixed, the rate of change increases monotonically with the proportion of mobile users. The channels to mobile users experience more changes than the channels to fixed users. The results indicate that the overheads for tracking the interference environment might be scalable with user density but increase with user mobility. We further evaluate how such temporal variation influences the overheads in simple MAC clustering protocols akin to those in current standards [6]. We show that mobility would increase the time to form clusters, degrade the quality of signaling channels and cause more re-clustering. Our analysis results quantitatively support the conclusion that in a highly dynamic environment, if a node is to coordinate at all, it should focus on doing so with fixed users which are close by.

Related work. Channels in the mmWave bands are highly sensitive to user movements, including small local movements like the rotation of a torso or swinging and large scale movements, e.g., people walking around. Existing works on user mobility [9][10][11] study the influence of human activity on the radio channel between a fixed transmitter and receiver. For example, the authors of [9][10] present measurements of the impact of human mobility on channel variation. The authors of [10] further evaluate the probability that a channel is blocked by users and proposes a two-state Markov model for the state of the channel based on experiments. The authors of [11] use simulation to study radio propagation characteristics in the presence of static and moving obstacles and show that directional LOS mmWave links experience relatively high outage. These works provide valuable measurements and insights on the influence of blockages resulting from human mobility, but do not provide models towards understanding the impact of user mobility in dense environments, or towards understanding the impact of density on the conclusions.

The authors of [12] propose and evaluate link scheduling algorithms for mmWave ad hoc networks but the characteristics of their channel blockage model are arbitrarily set without accounting for actual blockage mobility models. The implications of MAC design for dense mmWave wearable networks are studied in [5] but large scale user mobility is not considered.

By contrast with previous works, this paper provides a new set of tools to help understand the impact of mobility on mmWave based networks, with a goal of understanding scalability, the associated overheads, and how robust MAC designs might be across a range of operational scenarios.

Organization. In Section II we present our system model and background results used to analyze mmWave wearable networks and user mobility. We study the temporal variation of the blocking state of a fixed channel in Section III and evaluate the rate of changes in channels to neighboring interferers in Section IV. We further explore the impact of mobility on MAC in Section V. We present the numerical results in Section VI and conclude the paper with Section VII.

II. Background Results and System Model

In this section we introduce our system model for a mmWave network with mobile users along with some fundamental background results that are critical to have a clear understanding of our work.

A. Background Notation and Key Results

We introduce some notations for set operations, see [13]. For $x \in \mathbb{R}^2$, $A, B \subset \mathbb{R}^2$,

$$A \oplus B = \{x + y : x \in A, y \in B\}, \tag{1}$$

$$x + B = \{x + y : y \in B\}, \tag{2}$$

$$\check{B} = \{x : -x \in B\}. \tag{3}$$

Here $\oplus$ denotes the Minkowski sum of sets.

The following results will be used repeatedly in the sequel and are fairly well known in the literature:

- Displacement Theorem in $\mathbb{R}^2$ [14]
- Boolean Model in $\mathbb{R}^2$ [15]
- Generalized Steiner Formula in $\mathbb{R}^2$ [15]

The above results provide the following key insights in the context of modeling mobile blockages. Displacement theorem indicates that starting with a Homogeneous Poisson Point Process (HPPP) of blockages locations, randomly displacing blockages gives another HPPP. If a set of blockages can be modeled as a Poisson Boolean Process in Boolean model, the number of such blockages intersecting a set follows a Poisson distribution. Generalized Steiner formula helps calculate the expected area of the Minkowski sum of random sets.

B. System Model

In a wearable network, each user is equipped with multiple wearable devices. The devices on each user are assumed to form a Personal Basic Service Set (PBSS), coordinated by the PBSS Control Point (PCP), e.g., the user's smart phone. Data transmissions only happen between the PCP and non-PCP devices of the same PBSS. We shall assume each user is equipped with a device, e.g., a smart phone, which serves as coordinator for the user's wearable devices. The coordinating device will be assumed to be located in front of the user's body. We shall use the channels amongst the centers of users to approximate the channels amongst devices associated with different users.

We shall consider networks composed of two types of users, fixed and mobile users. Due to the low transmit power and high

attenuation in the mmWave band, the maximum range of a potential interferer is limited in wearable networks, e.g., 10m. Consider a channel within this limited range, the movements of users/blockages can be approximated as constant velocity movements, i.e., the velocity and the direction of the blockages at that scale may be assumed to be fixed. We refer to this mobility model as the Constant Velocity Model (CVM)[1].

Channel model. We shall focus on LOS channels in this work. We also consider human bodies as the main source of blockages. Human body introduces more than 20dB path loss [16] thus we assume an LOS channel is unavailable if a human is in the way. In fact the blockage model in our analysis may also represent blockages other than human bodies. In the mmWave band, the path loss of NLOS channels are typically dominated by a few major reflected paths. The blockage of reflected channels over the floor and ceiling are typically also coupled with the blockage state of the LOS channel. For other reflected paths, e.g., reflection over the wall, we may assume they are independent of the LOS channel and can approximate their temporal variation using the model for LOS channels. However such NLOS channels are much weaker than the LOS channel due to longer path and reflection loss and are more likely to be blocked. In this initial work, we do not consider the diffraction of signals and NLOS channels. Self blockage is independent of other blockages thus in the sequel, we focus on the channels that are not self blocked by default. The impact of channel variation caused by self blockage and users' small local movements is studied in [5].

Location and shape of user cross section. We suppose the blockages are cylindrical and focus on the blockage on LOS channels. For simplicity we consider 2D model in our analysis. Suppose users are randomly located on $\mathbb{R}^2$ where the centers of fixed users are $\Phi^f = \{X_i^f\} \sim HPPP(\lambda^f)$ and centers of mobile users at time 0 are $\Phi^m = \{X_i^m\} \sim HPPP(\lambda^m)$. We further assume Φ^m is independent of Φ^f and mobile users' movements are independent, e.g., users can overlap with each other.

Denote by A_i^f (A_i^m) a random closed convex set modeling the shape of fixed (mobile) user i's cross section. $A_i^f(A_i^m)$ is centered at 0 and we denote by Θ_i^f (Θ_i^m) the random direction user i is facing. A_i^f, A_i^m are independent and identically distributed (IID) as are Θ_i^f, Θ_i^m, which are assumed to be uniformly distributed in $[0, 2\pi]$.

Mobility model. We let the random variable S_i^m model the speed of mobile user i, be IID, and such that $S_i^m \in [s_{\min}, s_{\max}]$ where $0 < s_{\min} \leq s_{\max} < \infty$. Mobile user i is assumed to move in its facing direction Θ_i^m. Denote by $W_i^m \in \mathbb{R}$ the width of mobile user i as viewed from the facing direction Θ_i^m, and $V_i^m \in \mathbb{R}^2$ its velocity vector, i.e.,

$$V_i^m = \left(S_i^m \cos\Theta_i^m, S_i^m \sin\Theta_i^m\right). \tag{4}$$

See Fig. 1a for an illustration of user body model. We shall further let $X_i^m(t)$ denote the location of the center of mobile user i at time t, $t \geq 0$, thus

$$X_i^m(t) = X_i^m + t \cdot V_i^m. \tag{5}$$

The mobility model here corresponds to scenarios where users' movements are independent and random, e.g., crowded airport/shopping mall. Our model and analysis can also be extended to other mobility models, e.g., blockages move in the same direction.

The locations, cross sections, facing directions and velocities, of fixed and mobile users at time 0 can be represented by two independent Independently Marked Poisson Point Processes (IMPPP) [15], $\tilde{\Phi}^f$ and $\tilde{\Phi}^m$, given by

$$\tilde{\Phi}^f = \{(X_i^f, A_i^f, \Theta_i^f)\},$$
$$\tilde{\Phi}^m = \{(X_i^m, A_i^m, \Theta_i^m, S_i^m)\}.$$

Denote by $\Phi^m(t)$ the point process representing the locations of mobile users at time t, $\tilde{\Phi}^m(t)$ the marked point process for mobile users at t. It follows immediately from the Displacement theorem [14] that $\Phi^m(t)$ is also an HPPP with intensity λ^m and we have the following proposition.

Proposition 1. *If users make constant velocity movements, $\tilde{\Phi}^m$ is an IMPPP with intensity λ^m and Θ_i^m and S_i^m are IID, then at any time t $\tilde{\Phi}^m(t)$ is an IMPPP with the same distribution.*

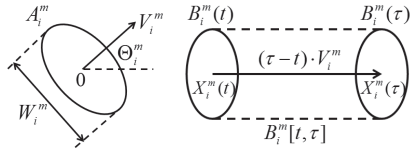

(a) User body. (b) User trace.

Fig. 1. (a) Model for mobile user i. A_i^m is centered at 0 and the actual cross section of mobile user i is $X_i^m + A_i^m$. $V_i^m = (S_i^m \cos\Theta_i^m, S_i^m \sin\Theta_i^m)$. (b) Trace of mobile user i in $[t, \tau]$, $B_i^m[t, \tau]$.

Blockage model. We shall for simplicity assume a channel is blocked if a blockage intersects the LOS channel between two devices. Let $x \in \mathbb{R}^2$ and $l_{0,x} \subset \mathbb{R}^2$ be the line segment between 0 and x, representing the LOS channel between the two points. We shall let B_i^f and B_i^m denote the region that fixed/mobile user i occupies at time 0, i.e.,

$$B_i^f = X_i^f + A_i^f \text{ and } B_i^m = X_i^m + A_i^m. \tag{6}$$

We further let $B_i^m(t)$ denote the region mobile user i occupies at time t, where

$$B_i^m(t) = B_i^m + t \cdot V_i^m = X_i^m(t) + A_i^m. \tag{7}$$

We say the channel between 0 and x is blocked at time t by mobile user i if $B_i^m(t) \cap l_{0,x} \neq \emptyset$ and for fixed user i if $B_i^f \cap l_{0,x} \neq \emptyset$.

Blockage traces. An important metric to capture interference temporal variation is the rate at which new blockages are seen by a channel. To compute these rates we shall determine if a mobile blockage i has blocked the channel in a given interval $[t, \tau]$, $t \leq \tau$, by defining the *blockage trace* in that time interval, denoted by $B_i^m[t, \tau]$ given by

$$B_i^m[t,\tau] = \bigcup_{t \leq z \leq \tau} B_i^m(z) = \bigcup_{t \leq z \leq \tau} \left(A_i^m + X_i^m(z)\right)$$
$$= A_i^m \oplus l_{X_i^m(t), X_i^m(\tau)} = X_i^m(t) + \left(A_i^m \oplus l_{0,(\tau-t)V_i^m}\right), \tag{8}$$

[1]Our analysis and results hold if the direction of movement is fixed while the speed changes.

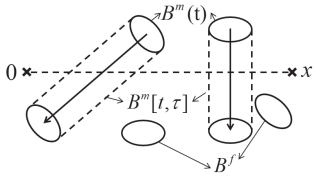

Fig. 2. Illustration of fixed blockages B^f, mobile blockages at time t, $B^m(t)$, and traces of mobile blockages in $[t,\tau]$, $B^m[t,\tau]$. B^f, $B^m(t)$ and $B^m[t,\tau]$ are Poisson Boolean Processes.

see Fig. 1b. Clearly mobile user i has blocked channel $l_{0,x}$ in $[t,\tau]$ if $B_i^m[t,\tau] \cap l_{0,x} \neq \emptyset$.

To estimate the number of blockages in $[t,\tau]$ using the generalized Steiner formula, we need the area and perimeter of $B_i^m[t,\tau]$. $A_i^m(t)$ is convex and $l_{X_i^m(t),X_i^m(\tau)}$ is a line segment, thus $\nu_2(B_i^m[t,\tau])$ and $\nu_1(B_i^m[t,\tau])$ are as follows,

$$\nu_2(B_i^m[t,\tau]) = \nu_2(A_i^m) + (\tau - t)S_i^m W_i^m, \tag{9}$$

$$\nu_1(\partial B_i^m[t,\tau]) = \nu_1(\partial A_i^m) + 2(\tau - t)S_i^m. \tag{10}$$

$B_i^m[t,\tau]$ can be viewed as stretching $B_i^m(t)$ by $(\tau - t)V_i^m$, the increase in area is $(\tau - t)S_i^m W_i^m$ and the increase in perimeter is $2(\tau - t)S_i^m$.

Boolean model. Denote by B^f the region covered by all fixed users, $B^m(t)$ the region covered by mobile users at time t, $B^m[t,\tau]$ the cumulative region covered by mobile users in the time interval $[t,\tau]$, i.e.,

$$B^f = \bigcup_{i=1}^{\infty} B_i^f = \bigcup_{i=1}^{\infty} \left(X_i^f + A_i^f\right), \tag{11}$$

$$B^m(t) = \bigcup_{i=1}^{\infty} B_i^m(t) = \bigcup_{i=1}^{\infty} \left(X_i^m(t) + A_i^m\right), \tag{12}$$

$$B^m[t,\tau] = \bigcup_{i=1}^{\infty} B_i^m[t,\tau] = \bigcup_{i=1}^{\infty} \left(X_i^m(t) + (A_i^m \oplus l_{0,(\tau-t)\cdot V_i^m})\right). \tag{13}$$

$\Phi^f, \Phi^m(t)$ are HPPPs, $A_i^f, A_i^m, A_i^m \oplus l_{0,(\tau-t)\cdot V_i^m}$ are IID random sets, thus B^f, $B^m(t)$ and $B^m[t,\tau]$ correspond to Poisson Boolean Process model [15], see Fig. 2.

Number of blockages. For a closed convex set $K \subset \mathbb{R}^2$, we denote by N_K^f the number of fixed users whose cross-sections intersect K, $N_K^m(t)$ the number of mobile users intersecting K at time t, $N_K^m[t,\tau]$ the cumulative number of mobile users that have intersected K in $[t,\tau]$, i.e.,

$$N_K^f = \sum_{i=1}^{\infty} \mathbb{1}(B_i^f \cap K \neq \emptyset), \tag{14}$$

$$N_K^m(t) = \sum_{i=1}^{\infty} \mathbb{1}(B_i^m(t) \cap K \neq \emptyset), \tag{15}$$

$$N_K^m[t,\tau] = \sum_{i=1}^{\infty} \mathbb{1}(B_i^m[t,\tau] \cap K \neq \emptyset) \tag{16}$$

Since B^f, $B^m(t)$ and $B_m[t,\tau]$ correspond to Poisson Boolean Processes, it follows by the Boolean model that N_K^f, $N_K^m(t)$ and $N_K^m[t,\tau]$ have Poisson distributions. Denote by A, Θ, S and W, random variables having the same distributions as A_i^f (A_i^m), Θ_i^f (Θ_i^m), S_i^m and W_i^m respectively. Θ is uniform in $[0, 2\pi]$ thus A is isotropic and $\mathrm{E}[\nu_2(K \oplus \check{A})]$ can be computed using the generalized Steiner formula. The expected number of blockages are given as follows,

$$\mathrm{E}[N_K^f] = \lambda^f \left(\nu_2(K) + \mathrm{E}\left[\nu_2(A)\right] + \frac{\mathrm{E}\left[\nu_1(\partial A)\right] \cdot \nu_1(\partial K)}{2\pi}\right), \tag{17}$$

$$\mathrm{E}[N_K^m(t)] = \lambda^m \left(\nu_2(K) + \mathrm{E}\left[\nu_2(A)\right] + \frac{\mathrm{E}\left[\nu_1(\partial A)\right] \cdot \nu_1(\partial K)}{2\pi}\right), \tag{18}$$

$$\mathrm{E}\left[N_K^m[t,\tau]\right] = \lambda^m \left(\nu_2(K) + \mathrm{E}\left[\nu_2(A)\right] + (\tau - t)\,\mathrm{E}[S]\,\mathrm{E}[W] + \frac{\left(\mathrm{E}[\nu_1(\partial A)] + 2(\tau - t)\,\mathrm{E}[S]\right) \cdot \nu_1(\partial K)}{2\pi}\right), \tag{19}$$

where we use the fact that for a convex set A, $\nu_2(\check{A}) = \nu_2(A)$, $\nu_1(\partial(\check{A})) = \nu_1(\partial A)$.

Strong interfering neighbor. User located at x is a strong channel to user at 0 if $l_{0,x}$ is unobstructed, i.e., an LOS channel, and $|x| \leq r_{\max}$, where $r_{\max}$ is the maximum length of a strong channel. If $|x| > r_{\max}$, we assume the channel is weak and user at 0 can ignore such a neighbor.

III. Time-varying Blocking for a Fixed Channel

Let us now consider the blocking state of fixed channels. Without loss of generality we consider the LOS channel between 0 and x, $l_{0,x}$, and denote by $|x|$ the length of $l_{0,x}$. The channel can be blocked by fixed and mobile blockages. We study the probability that the channel is blocked, then characterize the temporal variation in the blocking.

A. Probability of Having LOS Link

Denote by $\mathrm{P}_{l_{0,x}}^{\mathrm{LOS},f}$ the probability $l_{0,x}$ is not blocked by fixed blockages, $\mathrm{P}_{l_{0,x}}^{\mathrm{LOS},m}(t)$ the probability $l_{0,x}$ is not blocked by mobile blockages at t, $\mathrm{P}_{l_{0,x}}^{\mathrm{LOS}}(t)$ the probability $l_{0,x}$ is LOS at time t. For line segment $l_{0,x}$, $\nu_2(l_{0,x}) = 0$, $\nu_1(l_{0,x}) = 2|x|$, and the expected numbers of blockages for $l_{0,x}$ are given by,

$$\mathrm{E}[N_{l_{0,x}}^f] = \lambda^f \left(\mathrm{E}[\nu_2(A)] + \frac{\mathrm{E}[\nu_1(\partial A)] \cdot |x|}{\pi}\right), \tag{20}$$

$$\mathrm{E}[N_{l_{0,x}}^m(t)] = \lambda^m \left(\mathrm{E}[\nu_2(A)] + \frac{\mathrm{E}[\nu_1(\partial A)] \cdot |x|}{\pi}\right). \tag{21}$$

The probability of having LOS link is then given as follows,

$$\mathrm{P}_{l_{0,x}}^{\mathrm{LOS},f} = \mathrm{P}(N_{l_{0,x}}^f = 0) = e^{-\mathrm{E}[N_{l_{0,x}}^f]}, \tag{22}$$

$$\mathrm{P}_{l_{0,x}}^{\mathrm{LOS},m}(t) = \mathrm{P}(N_{l_{0,x}}^m(t) = 0) = e^{-\mathrm{E}[N_{l_{0,x}}^m(t)]}, \tag{23}$$

$$\mathrm{P}_{l_{0,x}}^{\mathrm{LOS}}(t) = \mathrm{P}_{l_{0,x}}^{\mathrm{LOS},f} \cdot \mathrm{P}_{l_{0,x}}^{\mathrm{LOS},m}(t) = e^{-\mathrm{E}[N_{l_{0,x}}^f] - \mathrm{E}[N_{l_{0,x}}^m(t)]}. \tag{24}$$

B. Temporal Variation of Fixed Channels

Next we consider the temporal variation of blocking caused by mobile users. Let us assume $l_{0,x}$ is not blocked by fixed users. Under our model, a mobile blockage moves in a fixed direction, thus each blockage blocks the channel at most once. A mobile user may start to block the channel, if so it blocks the channel for some time then stops blocking. We say a blockage

arrives at the channel if it begins to block the channel, i.e., the region the blockage intersects the channel. Denote by $T_i^m(l_{0,x}) \subset \mathbb{R}$ the (bounded) time interval mobile user i blocks channel $l_{0,x}$, i.e.,

$$T_i^m(l_{0,x}) = \{t \in \mathbb{R} \,|B_i^m(t) \cap l_{0,x} \neq \emptyset\}. \tag{25}$$

If the mobile user ever blocks the channel, i.e., $T_i^m(l_{0,x}) \neq \emptyset$, the mobile blockage i arrives at the channel at time $\min\{t|t \in T_i^m(l_{0,x})\}$ and leaves the channel at time $\max\{t|t \in T_i^m(l_{0,x})\}$. The duration of blocking is $|T_i^m(l_{0,x})|$.

The following theorem characterizes the temporal variation in blocking for $l_{0,x}$.

Theorem 1. *Under CVM model, if the LOS channel $l_{0,x}$ is not blocked by fixed users/blockages, the blocking of $l_{0,x}$ is an alternating renewal process. The length of an LOS period, $T_{l_{0,x}}^{\mathrm{LOS}}$, has an exponential distribution with mean*

$$\mathrm{E}[T_{l_{0,x}}^{\mathrm{LOS}}] = \frac{1}{\lambda^m \,\mathrm{E}[S]\big(\,\mathrm{E}[W] + 2|x|/\pi\big)}. \tag{26}$$

The length of an NLOS period, $T_{l_{0,x}}^{\mathrm{NLOS}}$, has mean

$$\mathrm{E}[T_{l_{0,x}}^{\mathrm{NLOS}}] = \frac{1 - \mathrm{P}_{l_{0,x}}^{\mathrm{LOS},m}(t)}{\mathrm{P}_{l_{0,x}}^{\mathrm{LOS},m}(t)}\,\mathrm{E}[T_{l_{0,x}}^{\mathrm{LOS}}], \tag{27}$$

where $\mathrm{P}_{l_{0,x}}^{\mathrm{LOS},m}(t)$ is given in Eq. 23.

To prove the theorem, we first prove the following lemma characterizing the arrivals of mobile blockages.

Lemma 1. *For a channel $l_{0,x}$ subject to CVM blockages, the arrival of mobile blockages follows a Poisson process with rate*

$$\lambda_{l_{0,x}}^Q = \lambda^m \,\mathrm{E}[S](\mathrm{E}[W] + 2|x|/\pi). \tag{28}$$

Proof. Denote by $N_{l_{0,x}}^{\mathrm{new}}(t,\tau]$ the number of blockages that arrive at $l_{0,x}$ during $(t,\tau]$, $\tau \geq t$. By Proposition 1, the mobile blockages follow an HPPP at time t. The movements of blockages are independent thus $N_{l_{0,x}}^{\mathrm{new}}(t,\tau]$ has a Poisson distribution. Based on our definition of $N_K^m[t,\tau]$, we have that

$$N_{l_{0,x}}^{\mathrm{new}}(t,\tau] = N_{l_{0,x}}^m[t,\tau] - N_{l_{0,x}}^m(t), \tag{29}$$

$$\mathrm{E}\left[N_{l_{0,x}}^{\mathrm{new}}(t,\tau]\right] = \mathrm{E}\left[N_{l_{0,x}}^m[t,\tau]\right] - \mathrm{E}\left[N_{l_{0,x}}^m(t)\right]. \tag{30}$$

Using Eq. 18 and 19, $\mathrm{E}[N_{l_{0,x}}^{\mathrm{new}}(t,\tau]]$ is given by,

$$\mathrm{E}\left[N_{l_{0,x}}^{\mathrm{new}}(t,\tau]\right] = \lambda^m \,\mathrm{E}[S]\big(\,\mathrm{E}[W] + 2|x|/\pi\big)(\tau - t). \tag{31}$$

For any time interval $(t,\tau]$, $N_K^{\mathrm{new}}(t,\tau]$ follows a Poisson distribution with mean proportional to $\tau - t$, thus the arrival of blockages follows a Poisson process [14]. We denote by $\lambda_{l_{0,x}}^Q$ the Poisson arrival rate of mobile blockages on link $l_{0,x}$, then we have, $\lambda_{l_{0,x}}^Q = \lambda^m \,\mathrm{E}[S]\big(\,\mathrm{E}[W] + 2|x|/\pi\big)$. □

Lemma 1 indicates, as might be expected, that the arrival rate of mobile blockages is proportional to blockage density λ^m and moving speed $\mathrm{E}[S]$. If we ignore the term for blockage width, $\mathrm{E}[W]$, the arrival rate is also proportional to link length. With Lemma 1, we can prove Theorem 1 as follows.

Proof of Theorem 1. We can model the channel as an $M/GI/\infty$ queue. The fixed channel can be viewed as an infinite server queue while mobile blockages are "jobs" that need service. The time that a blockage blocking the channel is "job" service time. By Lemma 1, mobile blockages follow Poisson arrival, which is memoryless (M). Furthermore, the typical time that a mobile user blocks the channel depends on the velocity and cross section of the blockage, thus has a general distribution (GI). By the CVM assumption, the movements of users are independent from each other and the time each mobile blockage blocks the channel is independent from others (infinite servers).

The state of the $M/GI/\infty$ queue captures whether the channel is LOS (on) or blocked NLOS (off), thus blocking can be modeled by an on/off renewal process, where $T_{l_{0,x}}^{\mathrm{LOS}}$ and $T_{l_{0,x}}^{\mathrm{NLOS}}$ are IID. In an $M/GI/\infty$ queue, the time that the queue is empty, which in our case is $T_{l_{0,x}}^{\mathrm{LOS}}$, follows an exponential distribution with mean $1/\lambda_{l_{0,x}}^Q$, i.e.,

$$\mathrm{E}[T_{l_{0,x}}^{\mathrm{LOS}}] = \frac{1}{\lambda^m \,\mathrm{E}[S]\big(\,\mathrm{E}[W] + 2|x|/\pi\big)}. \tag{32}$$

The distribution of the length of busy period, $T_{l_{0,x}}^{\mathrm{NLOS}}$, depends largely on the distribution of service time of each user, i.e., $|T_i^m(l_{0,x})|$, and is somewhat complex, see [17]. In CVM, the probability that the channel is not blocked by mobile users, $\mathrm{P}_{l_{0,x}}^{\mathrm{LOS},m}(t)$, is given in Eq. 23, thus we can compute $\mathrm{E}[T_{l_{0,x}}^{\mathrm{NLOS}}]$ without computing the exact distribution of $|T_i^m(l_{0,x})|$. For a renewal process, we have the following relationship among $\mathrm{P}_{l_{0,x}}^{\mathrm{LOS},m}(t)$, $\mathrm{E}[T_{l_{0,x}}^{\mathrm{LOS}}]$ and $\mathrm{E}[T_{l_{0,x}}^{\mathrm{NLOS}}]$,

$$\mathrm{P}_{l_{0,x}}^{\mathrm{LOS},m}(t) = \frac{\mathrm{E}[T_{l_{0,x}}^{\mathrm{LOS}}]}{\mathrm{E}[T_{l_{0,x}}^{\mathrm{LOS}}] + \mathrm{E}[T_{l_{0,x}}^{\mathrm{NLOS}}]}, \tag{33}$$

from which we can derive Eq. 27 □

The author of [18] shows that as job arrival rate goes to infinity, the busy period of $M/GI/\infty$ queue is asymptotically exponential with mean equal to expected busy period if the distribution function of service time, H, satisfies that,

$$(\log z)\int_z^\infty \{1 - H(y)\}\mathrm{d}y \to 0, \tag{34}$$

as $z \to \infty$. For our CVM model, we have the following result on the distribution of $T_{l_{0,x}}^{\mathrm{NLOS}}$.

Theorem 2. *In CVM, the distribution of $T_{l_{0,x}}^{\mathrm{NLOS}}$ approximates exponential distribution with mean $\mathrm{E}[T_{l_{0,x}}^{\mathrm{NLOS}}]$ as $\lambda_{l_{0,x}}^Q \to \infty$, i.e, λ^m, $\mathrm{E}[S]$, and/or $|x|$ goes to infinity.*

Proof. $S_i^m \geq s_{\min} > 0$, thus $|T_i^m(l_{0,x})|$ is upper bounded by $(|x| + d_A)/s_{\min}$, where d_A is the diameter of the smallest circle that contains A. $H(y) = 1$ for $y > (|x| + d_A)/s_{\min}$ thus Eq. 34 is satisfied. By Theorem 1 in [18], as $\lambda_{l_{0,x}}^Q \to \infty$,

$$\mathrm{P}\big(T_{l_{0,x}}^{\mathrm{NLOS}} \leq z\,\mathrm{E}\left[T_{l_{0,x}}^{\mathrm{NLOS}}\right]\big) \to 1 - e^{-z}, z > 0. \tag{35}$$

□

The key idea of Theorem 2 is that exponential distribution is a good approximation for the tail distribution of $T_{l_{0,x}}^{\mathrm{NLOS}}$ if

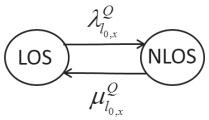

Fig. 3. Two-state continuous time Markov model for temporal variation of link $l_{0,x}$, which is not blocked by fixed users.

$\lambda^Q_{l_{0,x}}$ is large. By Lemma 1, $\lambda^Q_{l_{0,x}}$ is large if user density is high, user speed is large and/or channel is long. There are potential problems with approximating the distribution of $T^{\rm NLOS}_{l_{0,x}}$ with an exponential distribution. If $\lambda^Q_{l_{0,x}}$ is small, the exponential distribution may not fit $T^{\rm NLOS}_{l_{0,x}}$ well. The probability that the channel is blocked by more than one blockage is small and the distribution of $T^{\rm NLOS}_{l_{0,x}}$ is close to the conditional distribution of $|T^m_i(l_{0,x})|$ given $|T^m_i(l_{0,x})| > 0$. If $\lambda^Q_{l_{0,x}}$ is large, the assumption that user movements are independent and users can overlap may not be accurate.

If, for tractability, we approximate the distribution of $T^{\rm NLOS}_{l_{0,x}}$ with an exponential distribution with mean $\mathrm{E}[T^{\rm NLOS}_{l_{0,x}}]$, then the blocking of the channel becomes a renewal process with $T^{\rm LOS}_{l_{0,x}}$ and $T^{\rm NLOS}_{l_{0,x}}$ having exponential distributions, which can be modeled by a two-state continuous time Markov model [10], see Fig 3. The rate that the channel changes from LOS to NLOS is $\lambda^Q_{l_{0,x}}$, while the rate channel changes from NLOS to LOS $\mu^Q_{l_{0,x}}$ is,

$$\mu^Q_{l_{0,x}} = \mathrm{E}[T^{\rm NLOS}_{l_{0,x}}]^{-1}. \tag{36}$$

IV. Rate of Change for Strong LOS Neighbors Seen by Typical Receiver

In this section we study how the aggregate rate at which blocked/weak LOS neighbors change into strong LOS neighbors as seen by a typical fixed "reference" user. In principle, when a user becomes a strong LOS neighbor, the reference user needs to make channel measurements and initiate keeping track of that user. Thus the overall rate of change is a reasonable proxy for signaling overheads and the stability of the links the reference user sees.

We define the rate of change as seen by a reference user located at 0 at time t as follows. Denote by $N_0^{\rm change}[t,\tau]$ the number of users that became strong LOS neighbors of the reference user at 0 during $[t,\tau]$, given the fixed users $\tilde{\Phi}^f$ and mobile users $\tilde{\Phi}^m$. The mean rate of change as seen by the reference user, $f^{\rm total}$, is defined by

$$f^{\rm total} = \lim_{\tau\to t^+} \frac{\mathrm{E}_{\tilde{\Phi}^f,\tilde{\Phi}^m}\left[N_0^{\rm change}[t,\tau]\right]}{\tau - t}. \tag{37}$$

Based on our CVM model, $f^{\rm total}$ is invariant to t and can be characterized as follows.

Theorem 3. *Under CVM model, the rate of change for strong LOS neighbors seen by a typical fixed user, $f^{\rm total}$, is given by*

$$f^{\rm total} = f^{\rm range} + f^{\rm fixed} + f^{\rm mobile}, \tag{38}$$

where $f^{\rm range}$ is the rate at which mobile users enter $b(0,r_{\max})$, circle centered at 0 with radius $r_{\max}$, and have LOS channels, i.e, are not blocked, $f^{\rm fixed}$ is the rate of change associated with temporal variations in channels to other fixed users in $b(0,r_{\max})$, and $f^{\rm mobile}$ is the rate of change associated temporal variations in channels to mobile users in $b(0,r_{max})$. These three contributions are characterized as follows:

$$f^{\rm range} = 2\lambda^m r_{\max}\,\mathrm{E}[S]\mathrm{P}^{\rm LOS}_{l_{0,(0,r_{\max})}}, \tag{39}$$

$$f^{\rm fixed} = \lambda^f \int_{b(0,r_{\max})} \mathrm{P}^{\rm LOS}_{l_{0,x}}\lambda^Q_{l_{0,x}}\,dx, \tag{40}$$

$$f^{\rm mobile} = \lambda^m \int_{b(0,r_{\max})}\int_\theta\int_s \big(\delta^{\rm LOS}_{(x,\theta,s)} + \mathrm{P}^{\rm LOS}_{l_{0,x}}\cdot\big(\lambda^{Q,f}_{(x,\theta,s)} + \lambda^{Q,m}_{(x,\theta,s)}\big)\big)P_m(ds,d\theta)\,dx, \tag{41}$$

where $P_m(S,\Theta)$ is the probability measure of S and Θ, $\delta^{\rm LOS}_{(x,\theta,s)}$ is the rate that $\mathrm{P}^{\rm LOS}_{l_{0,x}}$ changes due to movement, $\lambda^{Q,f}_{(x,\theta,s)}$ and $\lambda^{Q,m}_{(x,\theta,s)}$ are the expected rate over $\tilde{\Phi}^f$ and $\tilde{\Phi}^m$, that the channel between the reference fixed user at 0 and a mobile user at location x with orientation θ and speed s, i.e., (x,θ,s), sees new blockages as a result of other fixed users and mobile users respectively.

$$\delta^{\rm LOS}_{(x,\theta,s)} = -(\lambda^f+\lambda^m)\cdot s\cdot\cos(\omega)\frac{\mathrm{E}\left[\nu_1(\partial A)\right]}{\pi}, \tag{42}$$

$$\lambda^{Q,f}_{(x,\theta,s)} = \lambda^f s\left(\frac{|x|\cdot|\sin(\omega)|}{2} + \frac{\mathrm{E}[\nu_1(\partial A)]}{\pi}\big(1+\cos(\omega)\big)\right), \tag{43}$$

$$\lambda^{Q,m}_{(x,\theta,s)} \approx \lim_{\tau\to t^+}\frac{\lambda^m\,\mathrm{E}_{A,V}\left[\nu_2\big(\check{A}\oplus M_{(x,v,V,\tau-t)}\big)\right]}{\tau-t}. \tag{44}$$

ω is the angle between v and vector from 0 to x, see Fig. 4a, $M_{(x_0,v_0,v,\tau-t)} = l_{0,x_0}\cup\big(-(\tau-t)\cdot v + l_{0,x_0+(\tau-t)\cdot v_0}\big)$, see Fig. 4b.

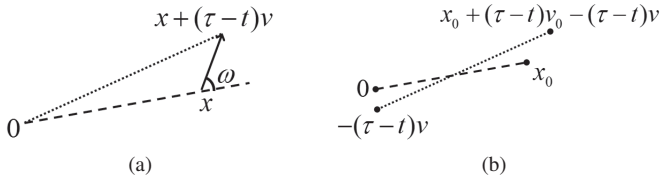

Fig. 4. (a) Movement of user at x with velocity v in$[t,\tau]$. ω is the angle between v and vector 0 to x. (b) Illustration of $M_{(x_0,v_0,v,\tau-t)}$.

The detailed proof is omitted due to space limits. Theorem 3 can also be extended for the rate of change seen by mobile users. If self blockage is considered, the rate of change becomes $p_{\rm facing}f^{\rm total}$, where $p_{\rm facing}$ is the probability that the channel between two users is not self blocked given that users are facing random directions. Actually $f^{\rm range}$ is not proportional to $p_{\rm facing}$, but it is small compared to $f^{\rm change}$, see Section VI.

V. Impact on MAC in mmWave Networks

In this section, we analyze the impact of temporal variation caused by mobility on MAC scheduler in mmWave wearable networks. In particular, we focus on a simple clustering based MAC design [5][6]. Fixed users form clusters with close by neighbors while mobile users work independently and do not

cooperate with each other. In each cluster, a user is selected as cluster head, which synchronizes cluster members, schedules signaling transmissions and coordinates data transmissions. Such a MAC involves formation and maintenance of clusters, and we study how user mobility would impact the overhead and performance of these two procedures.

We consider two scenarios, 1) a fixed user joins a network and connects to the closest strong LOS cluster head it finds within a probing interval, and 2) a user performs re-clustering after losing the strong LOS channel to cluster head for a given period time. The distribution of users is the same as described in Section II. Let us denote by M the average number of users in a cluster, and assume that each fixed user has a probability of $1/M$ to be a cluster head. As a simple model, we assume the locations of cluster heads follow an HPPP with density λ^f/M. We assume the state of channels are independent, and we use the two-state Markov model developed earlier to model the impact of dynamic blocking.

Joining Network. A randomly located fixed user joins the network at time 0. It scans the channel for some time t_{probe} and connects to the closest cluster head that it has strong LOS channel to during $[0, t_{\text{probe}}]$. We want to study the probability that the user finds at least one cluster head in $[0, t_{\text{probe}}]$ and the distribution of the distance to the cluster head it connects to. Use the location of the fixed user as the reference point 0, and denote by $\mathrm{P}^{\text{LOS}}_{l_{0,x}}[0, t_{\text{probe}}]$ the probability that $l_{0,x}$ has ever been LOS in $[0, t_{\text{probe}}]$, then we have

$$\mathrm{P}^{\text{LOS}}_{l_{0,x}}[0, t_{\text{probe}}] = \mathrm{P}^{\text{LOS},f}_{l_{0,x}} \cdot \left(1 - (1 - \mathrm{P}^{\text{LOS},m}_{l_{0,x}}(0)) \cdot e^{-\mu^{Q}_{l_{0,x}} \cdot t_{\text{probe}}}\right), \tag{45}$$

where $e^{-\mu^{Q}_{l_{0,x}} \cdot t_{\text{probe}}}$ is the probability the channel is kept blocked by mobile users in $[0, t_{\text{probe}}]$. Denote by $N^{\text{CH}}_{b(0,r)}(t_{\text{probe}})$ the number of cluster heads which are located in $b(0, r)$ and have an LOS channel to the new user in $[0, t_{\text{probe}}]$. Channels are independent thus $N^{\text{CH}}_{b(0,r)}(t_{\text{probe}})$ has a Poisson distribution with mean

$$\mathrm{E}\left[N^{\text{CH}}_{b(0,r)}(t_{\text{probe}})\right] = \frac{\lambda^f}{M} \int_{b(0,r)} \mathrm{P}^{\text{LOS}}_{l_{0,x}}[0, t_{\text{probe}}] dx. \tag{46}$$

Denote by D_{CH} the distance to the closest cluster head that user finds in $[0, t_{\text{probe}}]$, and $G_{D_{\text{CH}}}(\cdot)$ the cumulative density function (CDF) of D_{CH}. $N^{\text{CH}}_{b(0,r)}(t_{\text{probe}})$ has a Poisson distribution thus

$$G_{D_{\text{CH}}}(r) = \mathrm{P}\left(N^{\text{CH}}_{b(0,r)}(t_{\text{probe}}) \geq 0\right) = 1 - e^{-\mathrm{E}[N^{\text{CH}}_{b(0,r)}(t_{\text{probe}})]}. \tag{47}$$

The probability that the new user has found a cluster head in $[0, t_{\text{probe}}]$, $\mathrm{P}_{\text{connect}}(t_{\text{probe}})$, is $G_{D_{\text{CH}}}(r_{\max})$.

Re-clustering. We assume a user performs re-clustering if its channel to the cluster head is blocked for t_{out}. Assume the reference fixed user is located at 0, with the cluster head located at x. $l_{0,x}$ is LOS at time 0. Denote by $T^{\text{recluster}}_{l_{0,x}}$ the time before the user re-clusters. In Theorem 1 we have shown that the blocking of the channel is an alternating renewal process, thus re-clustering is performed if $T^{\text{NLOS}}_{l_{0,x}} \geq t_{\text{out}}$.

Denote by $\overline{G}_{T^{\text{NLOS}}_{l_{0,x}}}(t)$ the complementary CDF of $T^{\text{NLOS}}_{l_{0,x}}$, which is approximated by that of an exponential distribution with mean $\mathrm{E}\left[T^{\text{NLOS}}_{l_{0,x}}\right]$, see Eq. 27. The number of LOS periods before re-clustering is $1/\overline{G}_{T^{\text{NLOS}}_{l_{0,x}}}(t_{\text{out}})$, and the number of NLOS periods, excluding the NLOS period when re-clustering is performed, is $1/\overline{G}_{T^{\text{NLOS}}_{l_{0,x}}}(t_{\text{out}}) - 1$. The time with LOS channel before re-clustering is

$$\overline{G}_{T^{\text{NLOS}}_{l_{0,x}}}(t_{\text{out}})^{-1} \cdot \mathrm{E}\left[T^{\text{LOS}}_{l_{0,x}}\right],$$

and the time spent with no LOS connection to cluster head is

$$t_{\text{out}} + \left(\overline{G}_{T^{\text{NLOS}}_{l_{0,x}}}(t_{\text{out}})^{-1} - 1\right) \cdot \mathrm{E}\left[T^{\text{NLOS}}_{l_{0,x}} \middle| T^{\text{NLOS}}_{l_{0,x}} < t_{\text{out}}\right].$$

VI. Numerical Results and Design of MAC

In this section we evaluate the accuracy of our analysis and discuss the impact of mobile blockages on MAC design using numerical results. Users are assumed to have the same cross-sections, i.e., $0.45m \times 0.25m$ rectangles, with their facing directions perpendicular to the long side of the rectangle. User movements follow our CVM assumptions, the speed is $1\ m/s$ and $r_{\max}$ is $10\ m$.

Fig. 5 exhibits the CDF of $T^{\text{LOS}}_{l_{0,x}}$ and $T^{\text{NLOS}}_{l_{0,x}}$ for $\lambda^m = 0.5/m^2$. For $T^{\text{LOS}}_{l_{0,x}}$ our analysis is an exact match of simulation results. For $T^{\text{NLOS}}_{l_{0,x}}$ we can see that approximation using the two-state Markov model gives a good estimate for the distribution for large t, but not accurate for small t.

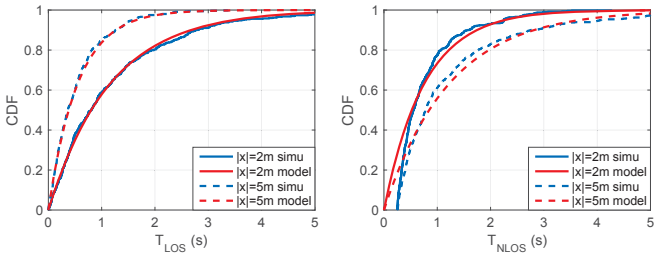

(a) CDF of $T^{\text{LOS}}_{l_{0,x}}$ (b) CDF of $T^{\text{NLOS}}_{l_{0,x}}$

Fig. 5. CDF of $T^{\text{LOS}}_{l_{0,x}}$ and $T^{\text{NLOS}}_{l_{0,x}}$, given $l_{0,x}$ is not blocked by fixed users.

Fig. 6 exhibits the rate of change as seen by a typical fixed user characterized in Theorem 3. In Fig. 6a, λ^f is the same as λ^m. In Fig. 6b, $\lambda^f + \lambda^m = 1$ user per m^2 while the proportion of mobile users, $\rho^m = \lambda^m/(\lambda^m + \lambda^f)$, changes. Comparing the analysis to the simulations shows that the analysis is a good match. From Fig. 6a we can see that as user density increases, the rate of change first increases due to increased mobility, then saturates and even begins decreasing. The reason is that in highly dense scenarios, most neighbors are blocked thus their impact on variability of the interference environment becomes limited. Also the rate of change contributed by mobile users is higher than that from fixed users. In Fig. 6b the rate of change increases almost linearly with the proportion of mobile users, ρ^m. The takeaway is that for dense environments, the channels may be poor due to blockage, but the overheads associated with tracking users may be limited at high densities. However, the overheads would increase with the proportion of mobile users. The design insight here is that fixed users may track other users when the proportion of mobile users is low. When the environment is highly mobile, i.e., with high proportion of

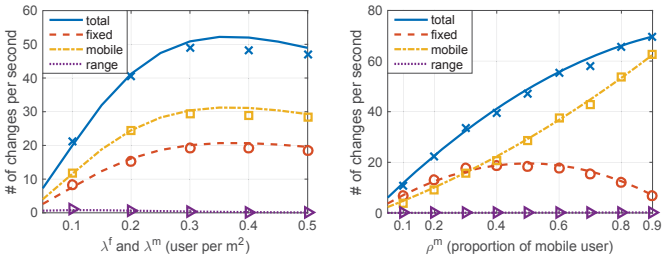

(a) Rate of change for $\lambda^f = \lambda^m$. (b) Rate of change for different ρ^m.

Fig. 6. Rate of change as seen by a typical fixed user. The markers represent results from simulations.

mobile users, users may choose not to coordinate with mobile users due to excessive overheads.

Fig. 7 exhibits results on a fixed user joining the network. As expected, $\mathrm{P}_{\mathrm{connect}}$ increases with t_{probe} while decreases with λ^m. The distribution of the distance to cluster head is pretty robust to t_{probe} and λ^m, but depends on the fixed user density λ^f and cluster size M. Such results indicate that clustering takes more time when there are more mobile blockages. The distance to cluster head, however, is not very sensitive to mobile blockages.

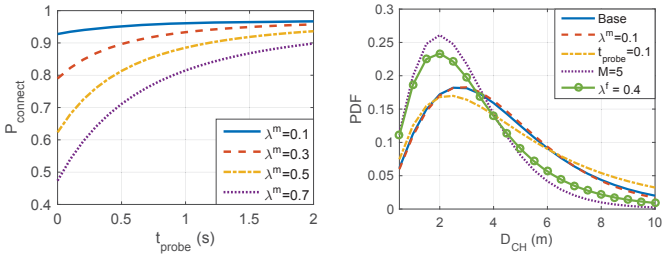

(a) Prob. finding cluster head in t_{probe} (b) PDF of distance to cluster head

Fig. 7. (a) Probability of finding a cluster head in $[0, t_{\mathrm{probe}}]$ and (b) the PDF of distance to the connected cluster head. In the Base case, $\lambda^f = 0.2/m^2$, $\lambda^m = 0.5/m^2$, $M = 10$, $t_{\mathrm{probe}} = 2s$.

Fig. 8 exhibits how mobile blockages impact re-clustering. As can be seen in Fig. 8a, the time before re-clustering grows super-linearly with t_{out}, indicating that a longer t_{out} can help reduce frequency of re-clustering. However, as shown in Fig. 8b, the channel to the cluster head is more likely to be blocked and the connection is poorer if t_{out} is larger. Choosing t_{out} requires making a trade-off between reducing re-clustering and improving connection quality for signaling. When λ^m is high, the frequency of re-clustering is high and the channel quality is poor, thus users should connect to closer cluster heads, or not use a coordination based MAC.

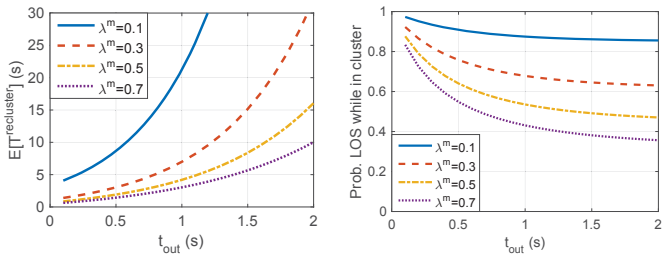

(a) Average time before re-clustering. (b) Proportion of time with LOS channel before re-clustering

Fig. 8. Impact of mobile blockages on re-clustering given $|x| = 4m$.

VII. Conclusion

This paper introduces a new model and analysis tools to study mobile blockages in mmWave settings where channel dynamics (LOS/NLOS) have an impact on MAC overheads/performance. Our formal results show the temporal variation between LOS/NLOS states of a channel is an on/off renewal process, whose holding time in each state is characterized. Based on our analysis, we derive the rate of change for channel states and estimate the associated signaling overheads resulting from user/blockage mobility. In dense and mobile networks, fixed users should perhaps track close by fixed users, and not be too reactive to changes due to blockages, most likely associated with moving users. Meanwhile, they should avoid coordinating with distant and/or mobile users. From a MAC perspective the challenge is to differentiate among mobile and fixed neighbors so as to optimize coordination and scheduling.

References

[1] "Smart Wearable Devices: Fitness, Glasses, Watches, Multimedia, Clothing, Jewellery, Healthcare & Enterprise 2014-2019," *Juniper Research*, Aug. 2014.

[2] H. Zhang, C. Wu, X. Cui, T. A. Guilliver, and H. Zhang, "Low Complexity Codebook-Based Beam Switching for 60 GHz Anti-Blockage Communication," *Journal of Communications*, vol. 8, no. 7, 2013.

[3] X. An, C.-S. Sum, R. Prasad, J. Wang, Z. Lan, J. Wang, R. Hekmat, H. Harada, and I. Niemegeers,"Beam Switching Support to Resolve Link-Blockage Problem in 60 GHz WPANs," in *PIMRC*, 2009.

[4] S. Sur, X. Zhang, P. Ramanathan and R. Chandra,"BeamSpy: Enabling. Robust 60 GHz Links Under Blockage," in *Proc. of NSDI*, 2016.

[5] Y. Wang and G. de Veciana, "Dense Indoor mmWave Wearable Networks: Managing Interference and Scalable MAC," in *WiOpt*, 2016.

[6] IEEE Standards Association,"IEEE Standards 802.11ad-2012: Enhancements for Very High Throughput in the 60 GHz Band," 2012.

[7] K. Venugopal, M. C. Valenti and R. W. Heath, *"Interference in Finite-Sized Highly Dense Millimeter Wave Networks,"* Information Theory and Applications Workshop, Feb. 2015.

[8] G. George and A. Lozano, "Performance of enclosed mmWave wearable networks," in *CAMSAP*, 2015.

[9] S. Collonge, G. Zaharia and G. E. Zein, "Influence of human activity on wide-band characteristics of the 60 GHz indoor radio channel," *IEEE Trans. Wirel. Commun.*, vol. 3, no. 6, pp. 2369-2406, 2004.

[10] I. Kashiwagi, T. Taga and T. Imai, "Time-varying path-shadowing model for indoor populated environments," *IEEE Trans. Veh. Technol.*, vol. 59, no. 1, Jan. 2010.

[11] S. Singh, F. Ziliotto, U. Madhow, E. M. Belding and M. Rodwell, "Blockage and Directivity in 60 GHz Wireless Personal Area Networks: From Cross-Layer Model to Multihop MAC Design," *IEEE J. Sel. Areas Commun.*, vol. 27, no. 8, Oct. 2009.

[12] Z. He, S. Mao and T. S. Rappaport, "On Link Scheduling Under Blockage and Interference in 60-GHz Ad Hoc Networks," *IEEE Access*, vol. 3, pp. 1437-1449, Aug. 2015.

[13] F. Baccelli and B. Blaszczyszyn, "Stochastic geometry and wireless networks, volume I - theory," *Foundations and Trends in Networking*, vol. 3, no. 3-4, pp. 249-449, 2009.

[14] J. F. C. Kingman, "Poisson Processes," New York: The Clarendon Press Oxford Univ. Press, 1993.

[15] S. N. Chiu, D. Stoyan, W. S. Kendall and J. Mecke, *Stochastic Geometry and its Applications* (3rd ed). Hoboken: Wiley, 2013.

[16] C. Gustafson and F. Tufvesson, "Characterization of 60 GHz shadowing by human bodies and simple phantoms," in *EuCAP*, 2012.

[17] P. Madadi, F. Baccelli and G. deVeciana, "On Temporal Variations in Mobile User SNR with Applications to Perceived QoS," in *WiOpt* 2016.

[18] P. Hall, "Heavy Traffic Approximations for Busy Period in an M/G/∞ Queue," *Stochastic Processes and their Applications*, vol. 19, no. 2, pp. 259-269, 1985.